Substrate composition directs slime molds behavior

Fernando Patino-Ramirez [1*], Aurèle Boussard[2], Chloé Arson[1¶], Audrey Dussutour[2¶*]

[1] School of Civil and Environmental Engineering, Georgia Institute of Technology, Atlanta, GA, USA

[2] Research Centre on Animal Cognition (CRCA), Centre for Integrative Biology (CBI), Toulouse University, CNRS, UPS, Toulouse, France

* Corresponding authors

E-mails: fp@gatech.edu (FP), audrey.dussutour@univ-tlse3.fr (AD)

¶ These authors contributed equally to this work.

Abstract

Cells, including unicellulars, are highly sensitive to external constraints from their environment. Amoeboid cells change their cell shape during locomotion and in response to external stimuli. Physarum polycephalum is a large multinucleated amoeboid cell that extends and develops pseudopods. In this paper, changes in cell behavior and shape were measured during the exploration of homogenous and non-homogenous environments that presented neutral, and nutritive and/or adverse substances. In the first place, we developed a fully automated image analysis method to measure quantitatively changes in both migration and shape. Then we measured various metrics that describe the area covered, the exploration dynamics, the migration rate and the slime mold shape. Our results show that: 1) Not only the nature, but also the spatial distribution of chemical substances affect the exploration behavior of slime molds; 2) Nutritive and adverse substances both slow down the exploration and prevent the formation of pseudopods; and 3) Slime mold placed in an adverse environment preferentially occupies previously explored areas rather than unexplored areas using mucus secretion as a buffer. Our results also show that slime molds migrate at a rate governed by the substrate up until they get within a critical distance to chemical substances.

Key words: Morphogenesis, Slime molds, Nutritive/adverse environments, Image analysis, Migration rate, Growth, Exploration

Author summary

Physarum polycephalum, also called slime mold, is a giant single-celled organism that can grow to cover several square meters, forming search fronts that are connected to a system of intersecting veins. An original experimental protocol allowed tracking the shape of slime mold placed in homogenous substrates containing an attractant (glucose) or a repellent (salt), or in homogeneous substrates that contained an attractive spot (glucose), an eccentric slime mold and a repulsive spot (salt) in between. For the first time, the rate of exploration of unexplored areas (primary growth) and the rate of extension in previously explored areas (secondary growth) were rigorously measured, by means of a sophisticated image analysis program. This paper shows that the chemical composition of the substrate has more influence on the morphology and growth dynamics of slime mold than that of concentrated spots of chemicals. It was also found that on a repulsive substrate, slime mold exhibits a bias towards secondary growth, which suggests that the mucus produced during slime mold migration acts as a protective shell in adverse environments.

Introduction

Large-scale spatial patterns in biology are common and knowing how these patterns evolve and what are their functional role, enables us to understand the evolution of biocomplexity (see e.g. (1–4)). Morphogenesis has been studied in length at the cell level (see e.g (5–8)); cells are highly sensitive to geometrical and mechanical constraints from their microenvironment and respond to these conditions by changing shape (see e.g. (9,10)); these transformations impact cell migration and growth (see e.g. (7,11–13)). Cellular migration is a fundamental property of every

cell and it is crucial for the development and morphogenesis of animal body plans and organ systems (see e.g. (14–16)). Cell migration is either in a random direction or directed towards localized cues (17–20). Mechanisms of cellular movement have been mostly studied in chemotactic cells, such as neutrophils (17), bacteria (21), Ciliata (22), fungi (23) and cellular slime molds (19).

Due to its extremely fast migration rate and highly irregular shape, the acellular slime mold *Physarum Polycephalum* represents a prime example of differentiated growth and thus offers an attractive model for the analysis of morphogenesis dynamics underlying cellular migration and exploration (24–28). *P polycephalum* is a giant single-celled organism that can grow to cover several square meters. Its morphology includes search fronts that are connected to a system of intersecting veins, in which oscillatory flows of the protoplasm “shuttle streaming” take place. This vein network allows 1) an efficient distribution of chemical signals, oxygen, nutrients over large distances and 2) cell migration at a speed of few centimeters per hour (29,30). The driving force for this protoplasm streaming is a periodic, peristaltic contraction and relaxation of the veins due to the actin-myosin interaction, which is regulated by oscillations of intracellular chemicals such as calcium (31–33). As it explores its environment, the slime mold extends temporary arm-like projections named pseudopods. It also secretes continuously a thick extracellular slime (34). The glycoprotein nature of the extracellular slime coat endows *P polycephalum* with unique protective and structural properties that favor survival of the migrating, naked slime mold (35). As the slime mold is foraging, it avoids areas covered with this mucus, which marks previously explored areas (36,37).

In the presence of chemical substances in the environment, *P. Polycephalum* shows directional movements towards or away from the stimuli (i.e. chemotaxis). *Physarum* morphology, evolution and behaviors are strongly affected by the availability, location and concentration of nutrients. When the slime mold senses attractants (e.g. food cues) using specific receptors located on the membrane, the oscillation frequency in the pseudopod closest to the attractant increases, causing cytoplasm to flow towards the attractant (38). On the contrary, when repellents such as salts are sensed, the oscillation frequency decreases and the slime mold moves away from the repellent (38). Although slime molds lack the complex hardware of animals with brains, they live in environments that are as complex and they face the same decision-making challenges (39). Hence, acellular slime molds have been the subject of a wide range of studies showing that they can solve complex biological and computational problems without any specialized nervous tissue (24,36,37,40–46).

In this paper the objectives are to characterize the morphology and dynamics of *Physarum* exploring various environments. First, we investigate how movement is affected by homogeneous environmental conditions: adverse environment (using salt as a repellent (47); nutritive environments (using glucose as a chemo-attractant (48,49) with 2 different concentrations) and a neutral environment (using plain agar). Second, we analyze the geometrical evolution of slime molds placed at a distance from a nutritive spot (glucose), with and without a repelling spot (salt) in between. We characterize slime molds' movement both temporally and spatially, to capture the full dynamics. To this aim, we develop a program that automatically analyzes sequences of images to track the areas covered and explored by the slime mold, the

slime mold shape, the refinement and secondary growth cycles, as well as the distance to the nutritive spot.

Results

1) Homogeneous environment

In order to study the influence of the environment on slime mold expansion rate, we analyzed the areas covered by slime mold, unexplored substrate and mucus over time, as shown in Fig 1.

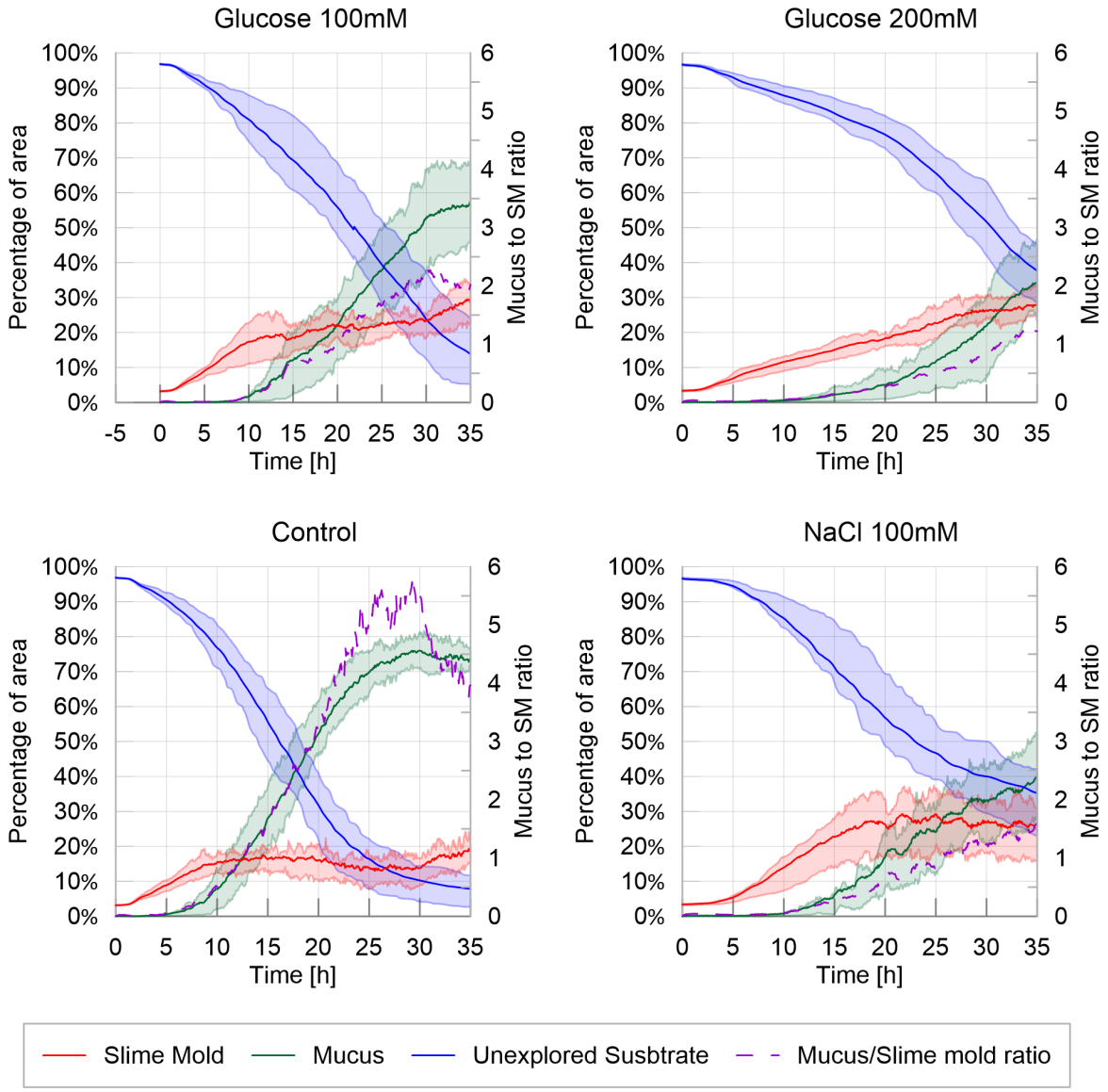

Fig 1. Fraction of area covered by slime mold, mucus and unexplored substrate – Homogeneous environment. The solid lines correspond to the average index calculated over the 20 replicates, while the shaded areas correspond to the first and third quartiles of the data, the dashed line correspond to the ratio between the average mucus area over the average slime mold area over time.

In a neutral (control) and slightly nutritive environment (glucose at 100 mM), the slime molds started to spread from the very beginning of the experiment (Fig 1; Table 1 and Fig 5 in S1 Appendix, $P>0.05$). By contrast, in a highly nutritive environment (200 mM glucose), slime molds started to explore later ($P<0.001$ when compared to the control). Slime molds placed in an adverse environment (100 mM NaCl) were lagging the most and only started exploring after 3 hours ($P<0.001$ when compared to the control). Once the slime molds started to explore, they all grew at the same rate (Fig 1; Table 2, Fig 6 in S1 Appendix, $P> 0.05$ when compared to the control) except the ones placed in a highly nutritive environment which were slowed down ($P<0.001$ when compared to the control).

At the end of the experiment (after 35 hours), the slime molds reached a similar surface area in a control environment and in an adverse environment (Table 3 and Fig 7 in S1 Appendix , $P>0.05$ when compared to the control). Interestingly, after reaching a plateau at 18 hours, the area covered by the slime molds in an adverse environment oscillated with seemingly cyclic fluctuations (Fig 1). In both a slightly and a highly nutritive environment, the slime molds reached a higher final surface area than the slime molds placed in a control environment ($P<0.001$ in both comparisons) and covered approximately 30% of arena at the end experiment. It is worth noting that in a highly nutritive environment, the area of the surface covered by the slime molds never reached a plateau after 35 hours, suggesting that the slime molds did not reach its maximum surface area (Fig 1).

Refinement *i.e.* appearance of mucus, was observed after 5 hours in the control environment. In all other environments, mucus appeared later (Table 4 and Fig 8 in S1 Appendix: $P<0.001$ for all treatments when compared to the control). In a highly nutritive environment, mucus was only observed after 10 hours, which marked the strongest delay in the refinement process. Once the mucus started to be apparent, its surface area grew quicker in the control environment than in the other three treatments (Table 5 and Fig 9 in S1 Appendix; $P<0.001$ for all treatments when compared to the control). Thus the area of the surface covered by mucus at the end of the experiment was the largest in the control environment where it reached 75% of the arena against 55%, 40% and 35% for the slightly nutritive, the adverse and the highly nutritive environments respectively (Table 6 and Fig 10 in S1 Appendix; $P<0.001$ for all treatments when compared to the control).

Hence, slime molds placed in a control environment explored almost all the arena leaving only 5% of the arena unexplored while in the other treatments the area of the surface unexplored were significant: 15%, 35% and 38% for the slightly nutritive, the highly nutritive and the adverse environments respectively. Interestingly, although the growth rate dynamics differed between highly nutritive and adverse environments, the final unexplored surface areas were similar. In a highly nutritive environment the slime molds grew slowly and steadily while in an adverse environment slime molds grew rather quickly but after a long delay.

Next, we analyzed the evolution of the cumulative areas covered by primary growth, refinement and secondary growth (Fig 2). The cumulative area covered by

secondary growth, which reveals the cyclic nature of the exploration process, was the highest in the adverse environment (480% coverage) followed by the control environment (380%), the slightly nutritive environment (250%) and the highly nutritive environment (180%). All comparisons lead to significant differences $P<0.05$, except control vs. adverse environment (Table 7 and Fig 11 in S1 Appendix). This observation confirms that exploration was slowed down by the presence of nutrients, and that the pulsatile behavior (*i.e* the exploration of previously explored area) was stimulated by repellents.

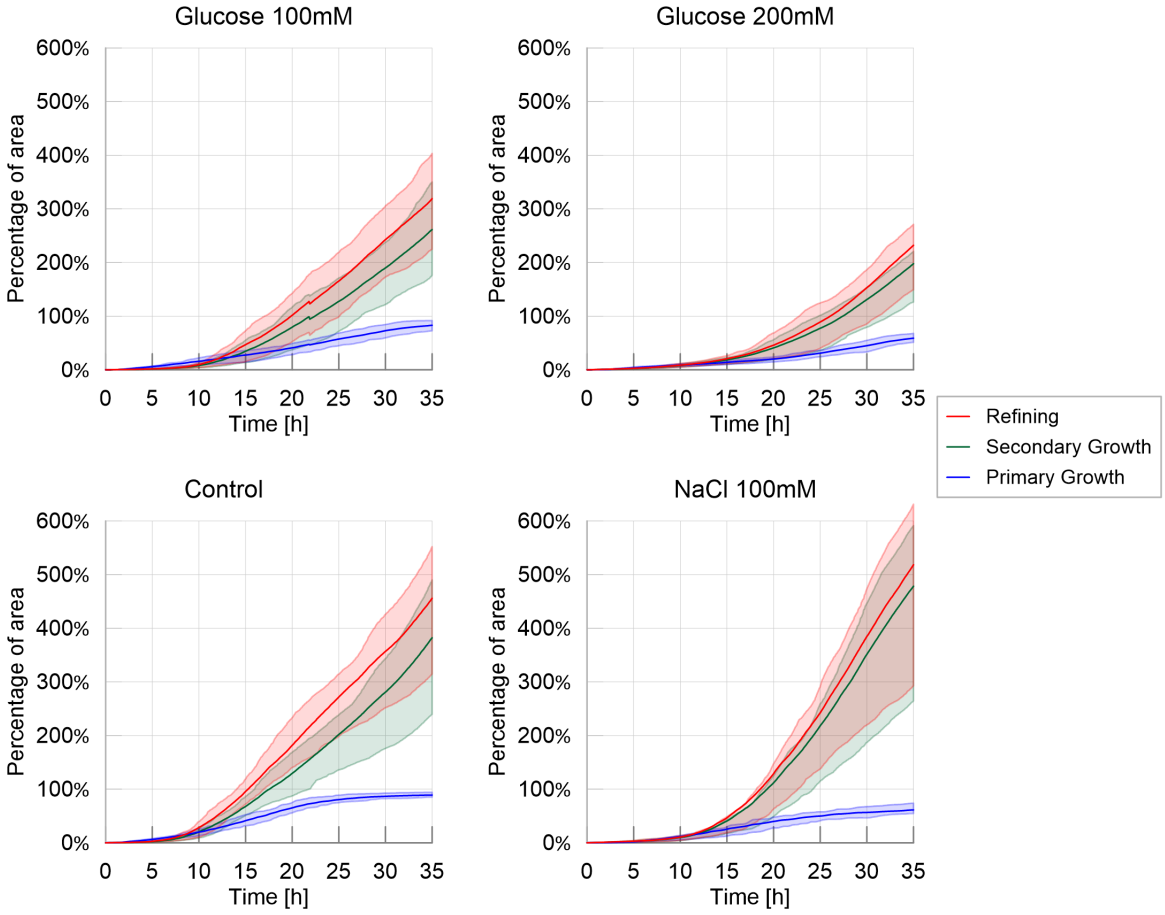

Fig 2. Cumulative areas covered by primary growth, refinement and secondary growth – Homogeneous experiments. The solid line corresponds to the average index calculated over the 20 replicates, while the shaded areas correspond to the first and third quartiles of the data.

In accordance with the previous results, the migration rate was higher for the control treatment than for the other treatments (Table 8 and Fig 12 in S1 Appendix: $P<0.001$ for each pairwise comparison). While slime molds exploring the highly nutritive environment were slower than slime molds exploring the slightly nutritive or the adverse environment ($P<0.001$ each), these two showed no significant differences ($P>0.05$).

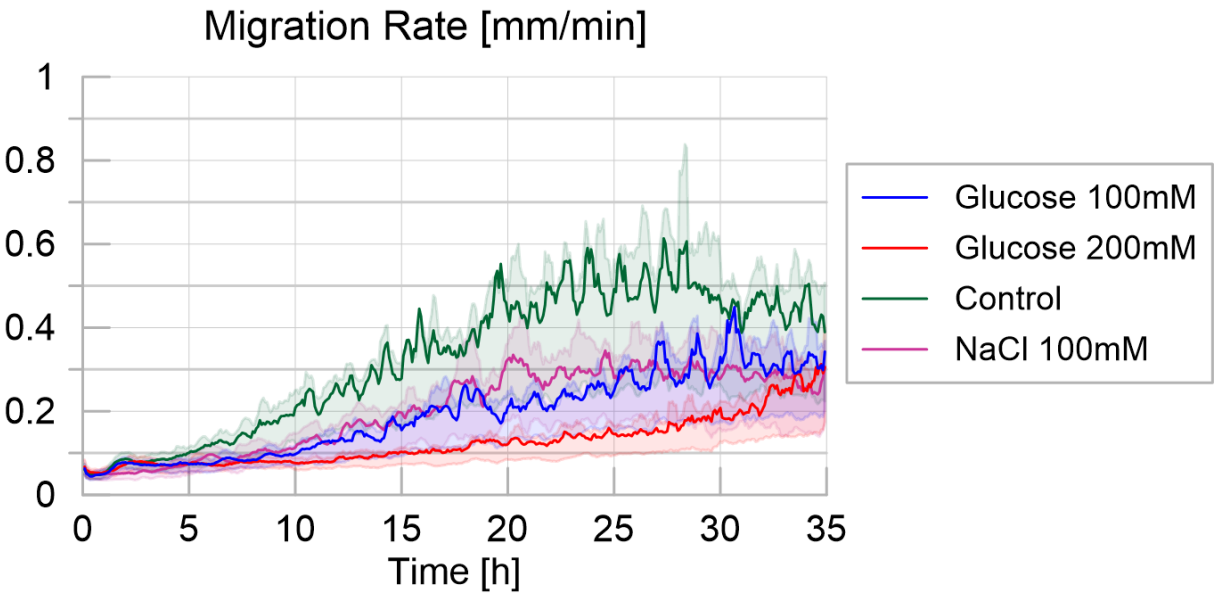

Fig 3: Migration rate over time for the four different treatments, defined as the maximum distance between the contours of the slime mold between two consecutive images divided by their time interval (5 minutes apart), measured in millimeters per minute. The solid line corresponds to the average calculated over 20 replicates per treatment, while the shaded areas correspond to the first and third quartiles of the data.

The slime molds exploring the adverse environment showed the highest probability to explore a previously explored substrate than the other treatments as shown in Fig 4 and supplementary materials (Tendency for secondary growth: Table 9 and Fig 13 in S1 Appendix: $P<0.001$ for each pairwise comparison). When exploring a highly

219 nutritive environment, slime molds also displayed a significant positive tendency for
220 secondary growth ($P<0.001$ for each pairwise comparison) but significantly less
221 strong than on the adverse environment ($P<0.001$). For the other treatments, the
222 measured proportion of secondary growth was not different from the expected
223 proportion of secondary growth, indicating that slime molds did not avoid previously
224 explored substrate and explored randomly (Fig 13 in S1 Appendix). The peaks
225 observed within the first 5 hours of the experiment correspond to an isotropic
226 extension immediately followed by a refinement process that occurred before the
227 slime mold started to explore continuously its environment. This behavior is often
228 observed when a slime mold is introduced in a new environment and is referred as
229 “contemplative” (50) *i.e.* the slime mold migrates, retracts and moves again. The
230 peak was larger in an adverse environment.
231

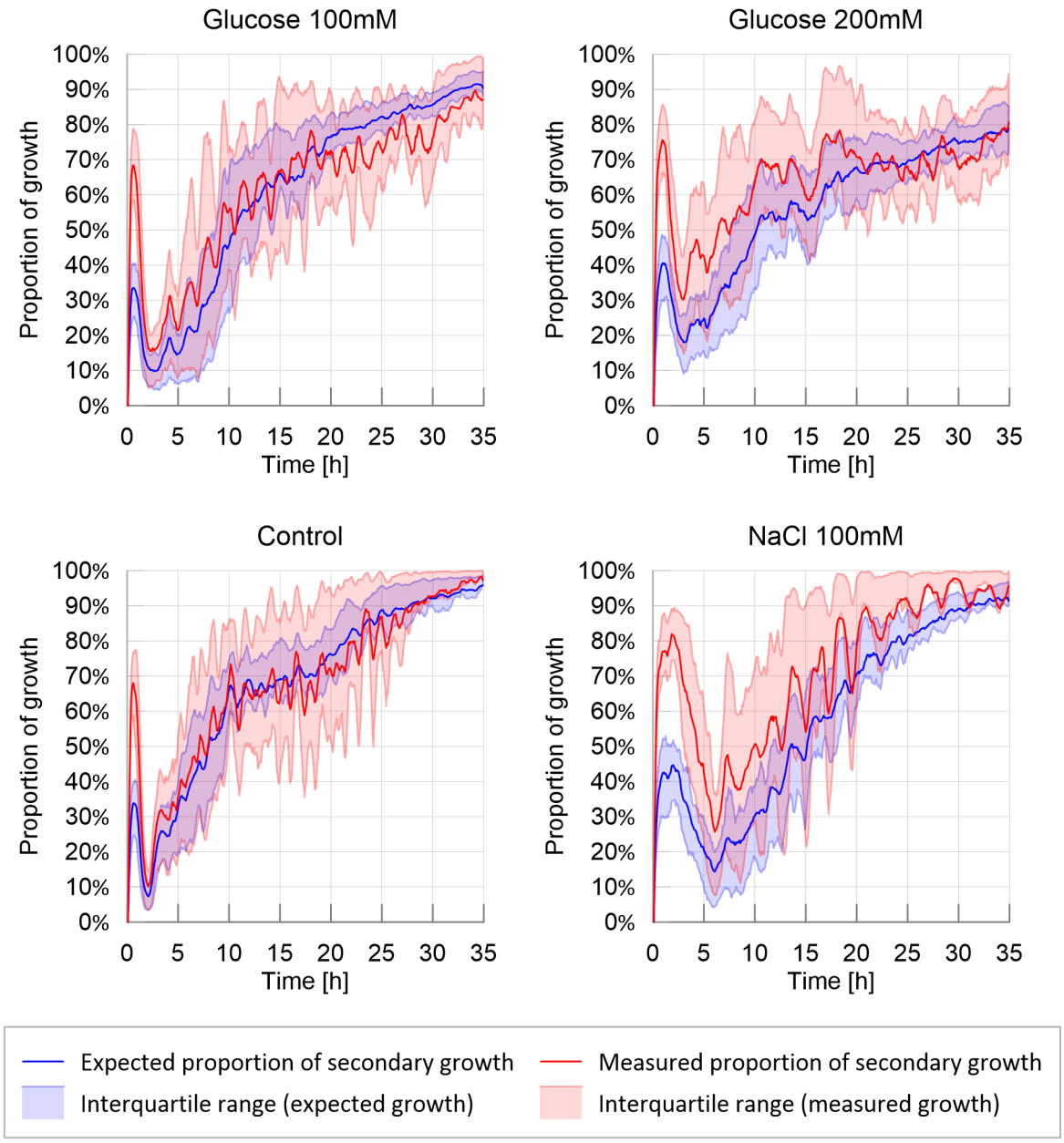

Fig 4: Ratio of secondary growth: observed and expected proportion of secondary growth. The solid line corresponds to the average calculated over 20 replicates per treatment, while the shaded areas correspond to the first and third quartiles of the data.

We then analyzed the evolution of the shape of the slime molds contour. Note that the experimental set ups in which slime molds were placed exhibited radial symmetry. Hence, no preferential expansion direction was expected. We thus focused on contour shape, not orientation.

As expected, circularity was initially one in all tests (circular slime mold spot), and increased over time as the contour shape departed from a circle (Fig 2 in S1 Appendix). In the control and nutritive environments, circularity remained between 1.05 and 1.10, whereas it fluctuated between 1.05 and 1.30 in the adverse environment. This observation suggests that, in an adverse environment, slime molds explored the petri dish by spreading and thinning over larger areas than in the other environments, which led to shape changes and a decrease of slime mold circularity. However fluctuations among the 20 replicates were too high to identify any trend in the evolution of slime mold circularity.

The eccentricity index was initially close to zero (circular cell) and increased up to almost 0.8 over time, with important fluctuations in all the treatments (Fig 3 in S1 Appendix). Eccentricity is an indicator of the number of pseudopodia. But a non-eccentric convex hull can enclose non-circular contours of slime mold, since pseudopodia can develop in a symmetric fashion. That is why no major difference was noted between the treatments. This result highlights the absence of preferred expansion direction in symmetric, homogeneous environments.

Solidity decreased with the emergence of pseudopodia, since slime mold branching disrupted the initially convex shape of the slime mold (Fig 5). In the control environment, in which the exploration rate was the highest, the decrease of solidity of the slime mold area was the highest (and the fastest) decreasing from 1 to 0.3 and then becoming relatively stable, with fluctuations of +/- 0.05 (Table 10 and Fig 14 in S1 Appendix; $P<0.01$ for all paired comparisons except adverse environment vs. slightly nutritive environment, where $P>0.05$). Slower exploration resulted in a slower and steadier loss of solidity as observed in the nutritive and adverse environments.

The highly nutritive environment yielded the highest solidity at the end of the experiment (0.6), which confirmed that the presence of glucose slowed down exploration.

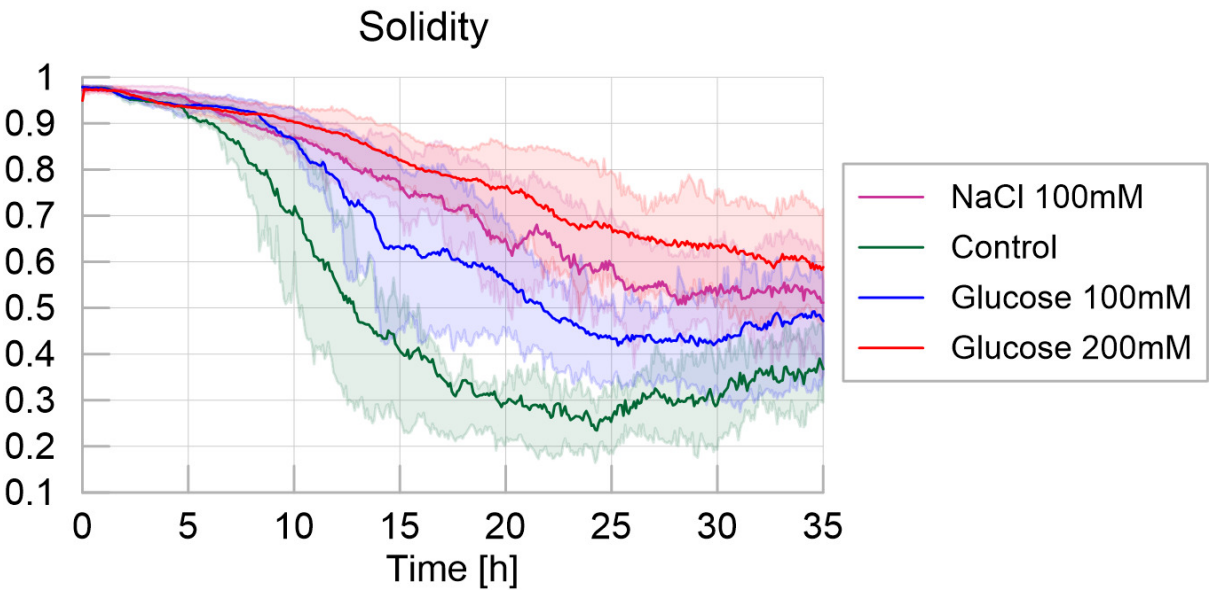

Fig 5. Solidity - Homogeneous experiments. The solid line corresponds to the average index calculated over the 20 replicates, while the shaded areas correspond to the first and third quartiles of the data.

We next focused on the number of clusters, corresponding to the number of pseudopodia (Fig 6). Initially the slime molds stretched as a single cluster. Once mucus started to be apparent, slime molds usually divided up into several clusters, and started the active exploration phase. In highly nutritive and adverse environments, the number of clusters over time was lower than in the other two treatments (new pseudopod number: Table 11 and Fig 15 in S1 Appendix, and $P < 0.01$ for all paired comparisons except for adverse environment vs. highly nutritive environment). This observation confirmed that the presence of concentrated nutrients slowed down the exploration, and that the presence of repellents triggered

a highly pulsatile behavior with small exploration fronts, which were sometimes not detected as separate clusters.

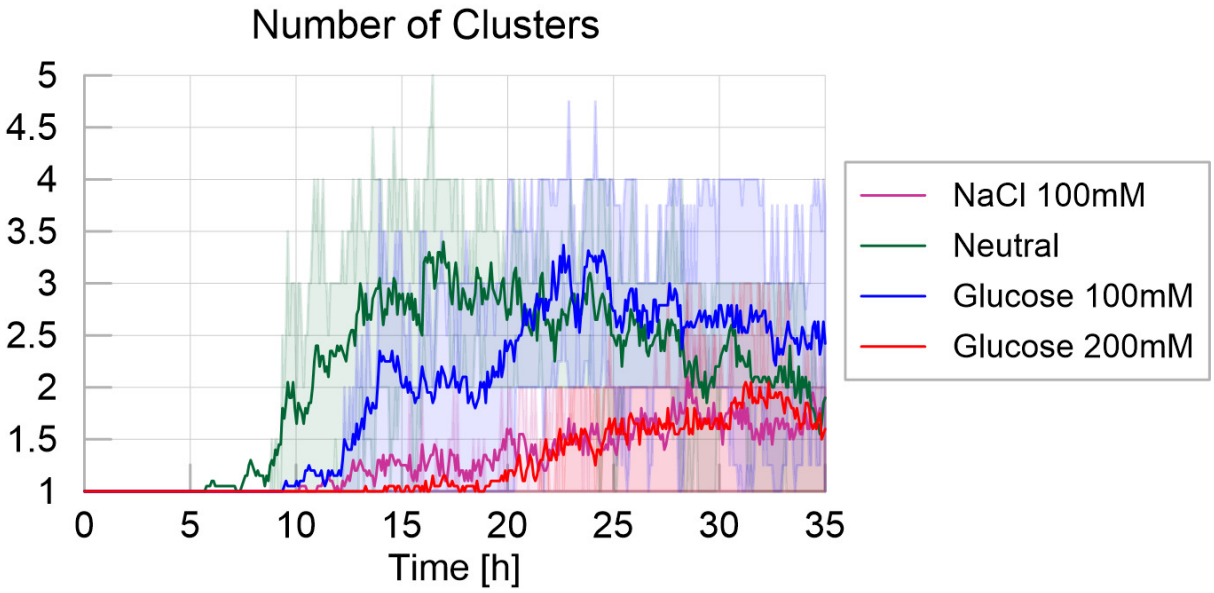

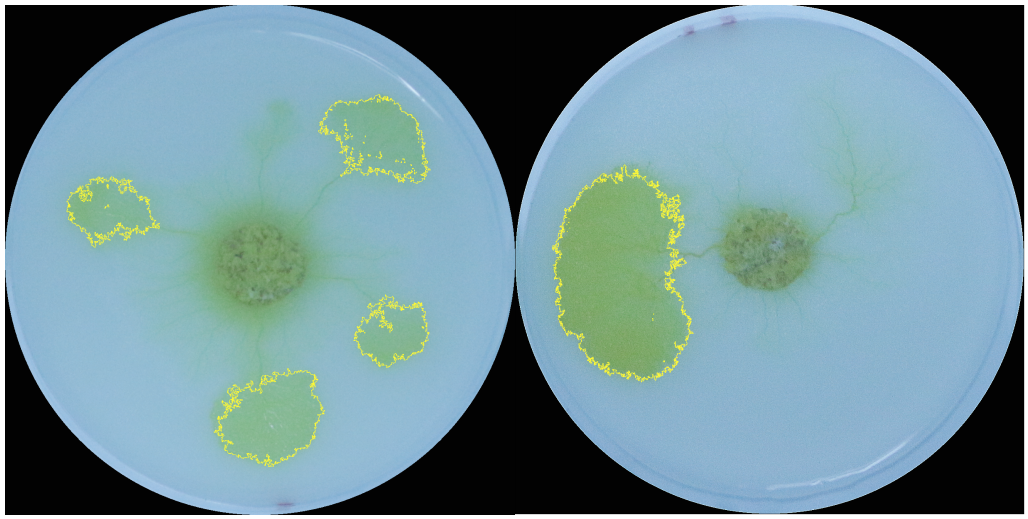

Fig 6. Number of clusters - Homogeneous experiments. The solid line corresponds to the average index calculated over the 20 replicates, while the shaded areas correspond to the first and third quartiles of the data. Pictures show examples of clusters for the Control environment (left) and 200mM Glucose environment (right).

296 **2) Spot experiments**

297 In the spot experiments, we studied the influence of discrete distributions of nutrients
298 and repellents on exploration dynamics. When looking at the evolution of slime mold,
299 mucus and unexplored substrate over time (Fig 7), we only observed marginal
300 difference among the treatments, which all exhibited similar patterns of exploration,
301 e.g. similar percentage of non-explored area and similar mucus accumulation. The
302 presence of an adverse spot only delayed the appearance of the first pseudopod
303 (first movement: Table 12 and Fig 15 in S1 Appendix, $P<0.05$) but not the first
304 appearance of mucus (first appearance of mucus: Table 15 in S1 Appendix, not
305 significant). The only noticeable differences lie in the surface area reached at the
306 end of the experiment: slime molds that were offered a highly nutritive spot grew
307 larger (final surface area: Table 14 and Fig 17 in S1 Appendix; $P < 0.01$). By
308 contrast, the area of the surface covered by mucus was lower (mucus final surface:
309 Table 17 and Fig 18 in S1 Appendix; $P <0.01$) than slime molds that were offered a
310 slightly nutritive spot. In comparison with the experiments conducted in
311 homogeneous environments, we did not observe any expansion/refinement cycles in
312 the spot experiments, meaning that slime mold spread steadily towards the food
313 source despite the presence of an obstacle on the way.
314

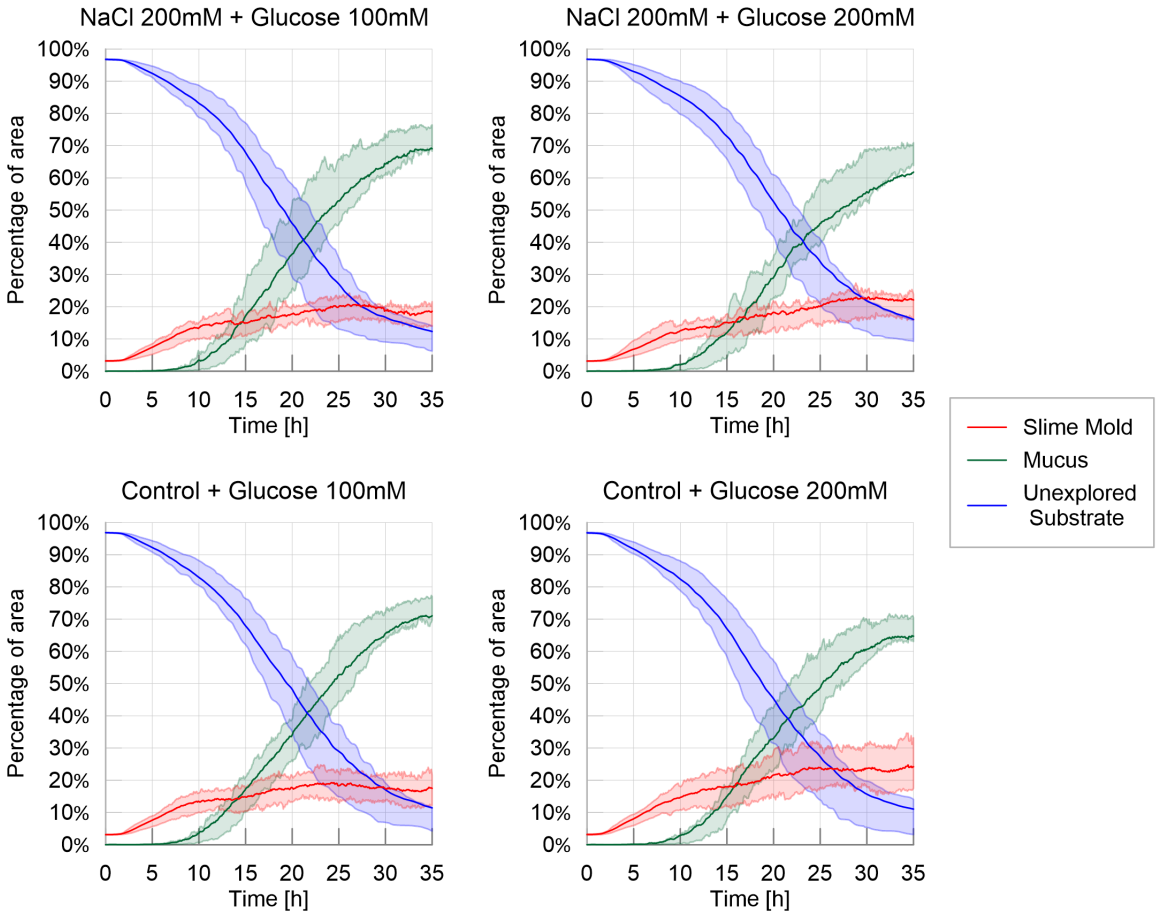

Fig 7. Fraction of area covered by each entity (slime mold, mucus, unexplored substrate) – Spot experiments. The solid line corresponds to the average index calculated over the 20 replicates, while the shaded areas correspond to the first and third quartiles of the data

The exploration behavior in the spot experiments was similar to that observed in the control environment in homogeneous experiments as observed in Fig 8, which includes the average percentage of unexplored area for the homogeneous and spot experiments shown in Fig 1 and Fig 7 respectively. This suggests that the spatial exploration of slime mold depended mostly on the substrate and not on the geometric distribution of the nutritive and adverse stimuli.

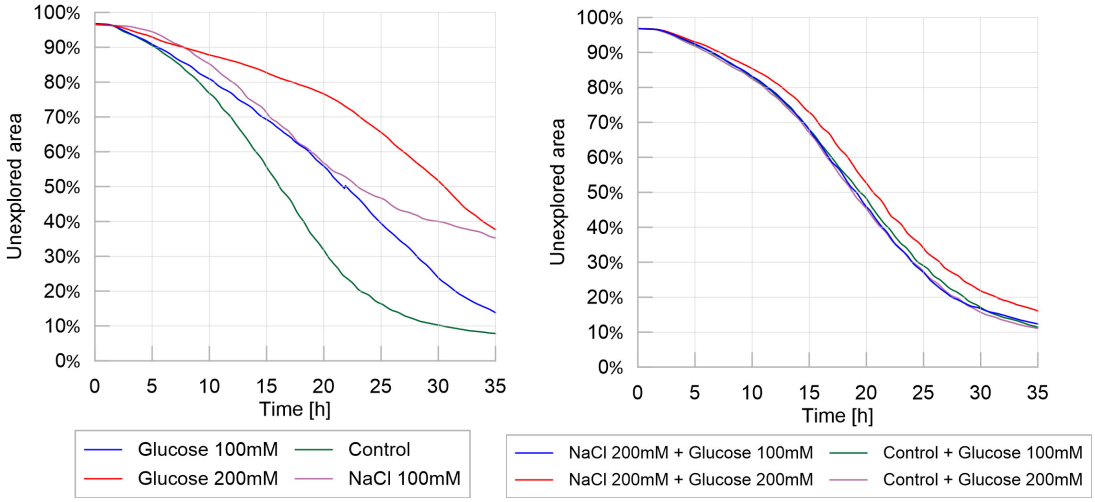

327

328 Fig 8. Exploration behavior: homogeneous experiments (left) vs. spot experiments (right). Percentage

329 of unexplored area over time. Mean values of over 20 replicates for each different treatment.

330

331 The cumulative areas covered by secondary growth for the spot experiments (Fig 9)

332 were also similar for all treatments (Table 18 in S1 Appendix, P >0.05), suggesting

333 again, that isolated spots with nutritive or adverse stimuli did not alter the overall

334 exploration of slime molds when growing on the same, control, substrate.

335

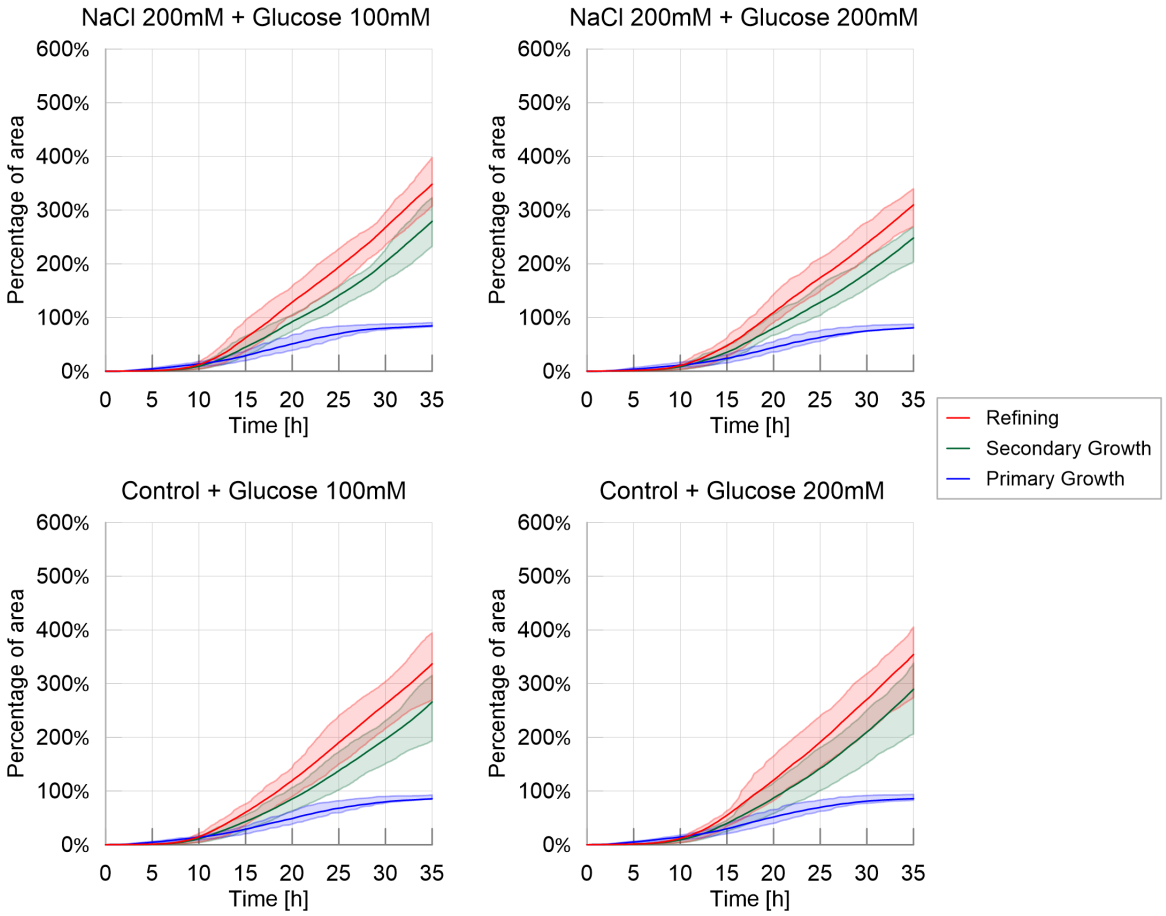

Fig 9. Cumulative areas covered by primary growth, refinement and secondary growth – Spot experiments. The solid line corresponds to the average index calculated over the 20 replicates, while the shaded areas correspond to the first and third quartiles of the data.

The trends of migration rate, as shown in Fig 10, show that slime molds were not affected by the difference between treatments, showing only a slight effect of the concentration of the food spot ($P<0.05$), as shown on Table 19 in S1 Appendix. This effect showed that the migration rate was slightly superior when slime molds were offered a higher than a lower nutritive spot.

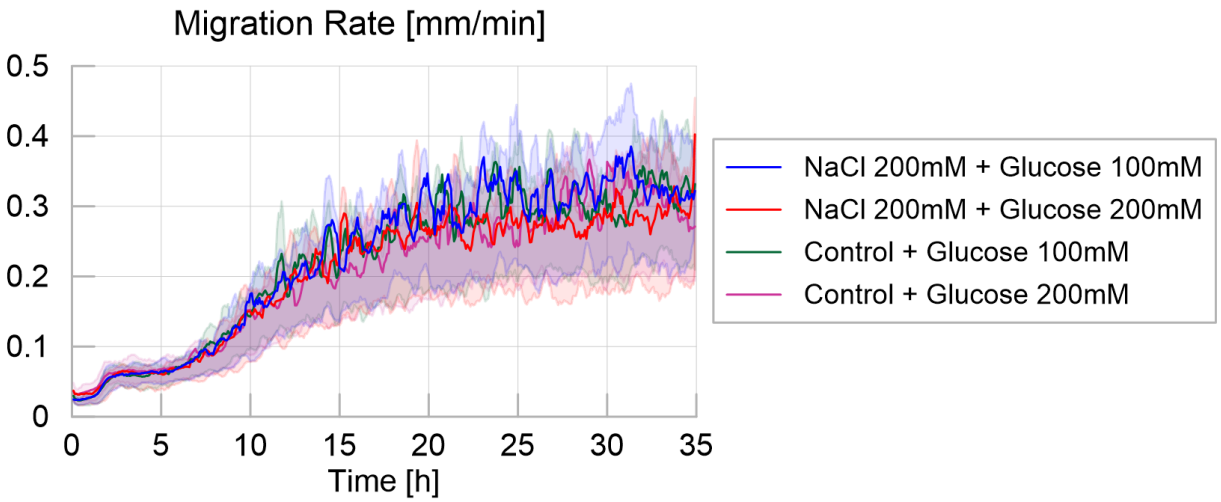

Fig 10: Migration rate over time for the four different treatments, defined as the maximum distance between the contours of the slime mold between two consecutive images, divided by their time interval (5 minutes apart), measured in millimeters per minute. The solid line corresponds to the average calculated over 20 replicates per treatment, while the shaded areas correspond to the first and third quartiles of the data.

Similarly, looking at the predilection of slime molds to grow towards mucus (secondary growth), as shown in Fig 11, no significant differences were observed between treatments (Table 19 in S1 Appendix), which suggests that the growth type is not influenced by the existence or concentration of discrete attracting/repelling spots.

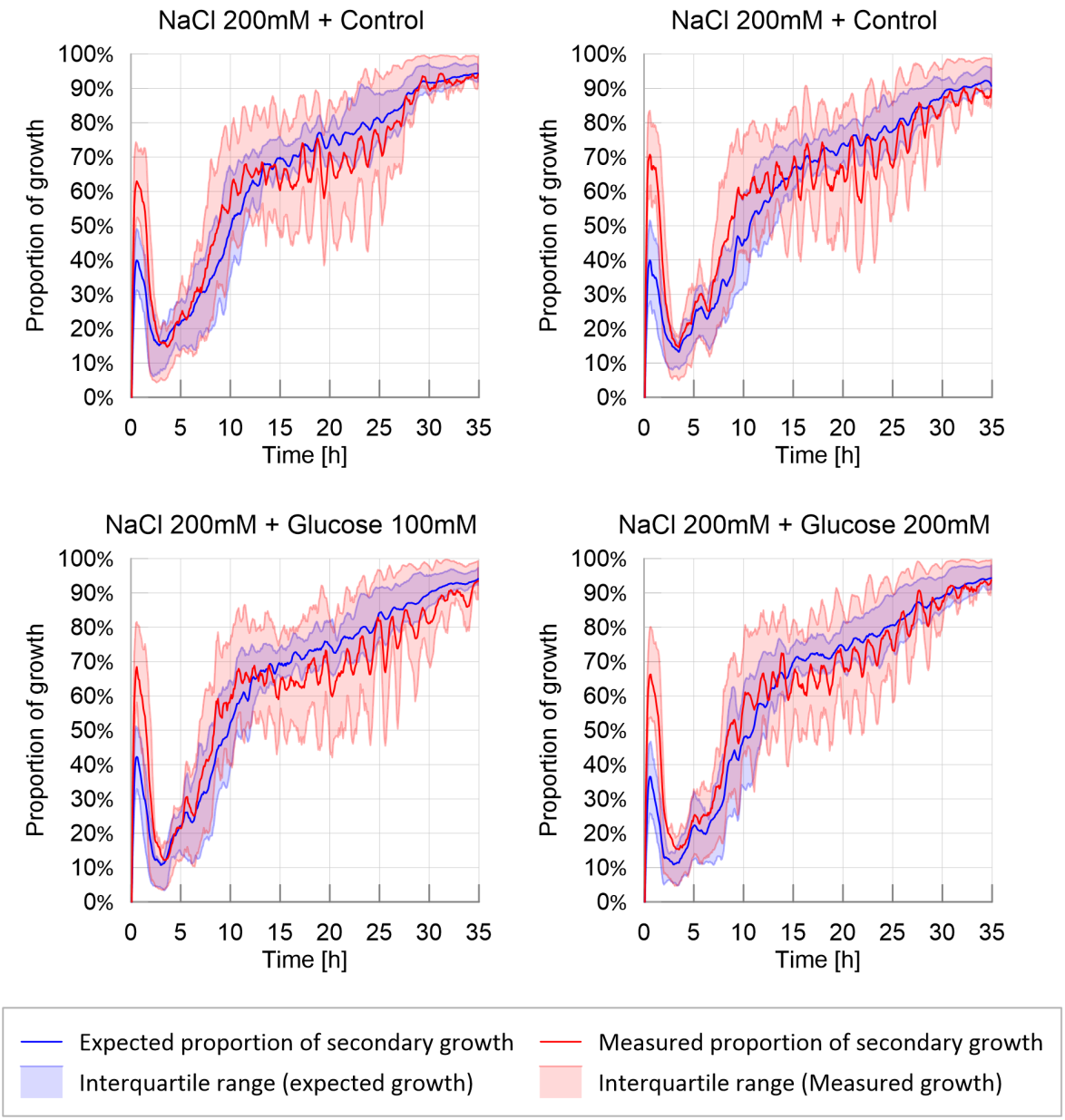

Fig 11: Probability of secondary growth: observed and expected proportion of secondary growth. The solid line corresponds to the average calculated over 20 replicates per treatment, while the shaded areas correspond to the first and third quartiles of the data.

The results obtained for the four different shape indexes (Fig 4 in S1 Appendix) for the spot experiments support the hypothesis that discrete spots of nutrients or repellents did not affect the overall expansion dynamics and exploration cycles. This interpretation is confirmed by the average number of pseudopods, which was found

to be correlated to the formation of mucus during the exploration phase: in all the spot experiments, the number of clusters increases from 1 to 2.5 within around 12 hours, to reach a plateau afterwards. In other words, less exploration cycles were observed in non-homogenous environments, yielding less pseudopodia.

The evolution of the shortest distance from the slime mold cell to the glucose spot is shown in Fig 12, which can be viewed as a “survival” plot, displaying the proportion of the replicate (P) in which slime mold has not reached the nutritive spot at a given time. Both increasing the concentration of nutrient in the spot (from slightly nutritive to highly nutritive) and adding an aversive spot increased the time to reach the food patch by decreasing the probability to reach it (time to food patch: Table 22 and Fig 18 in S1 Appendix, nutritive: $P< 0.01$; aversive: $P< 0.05$).

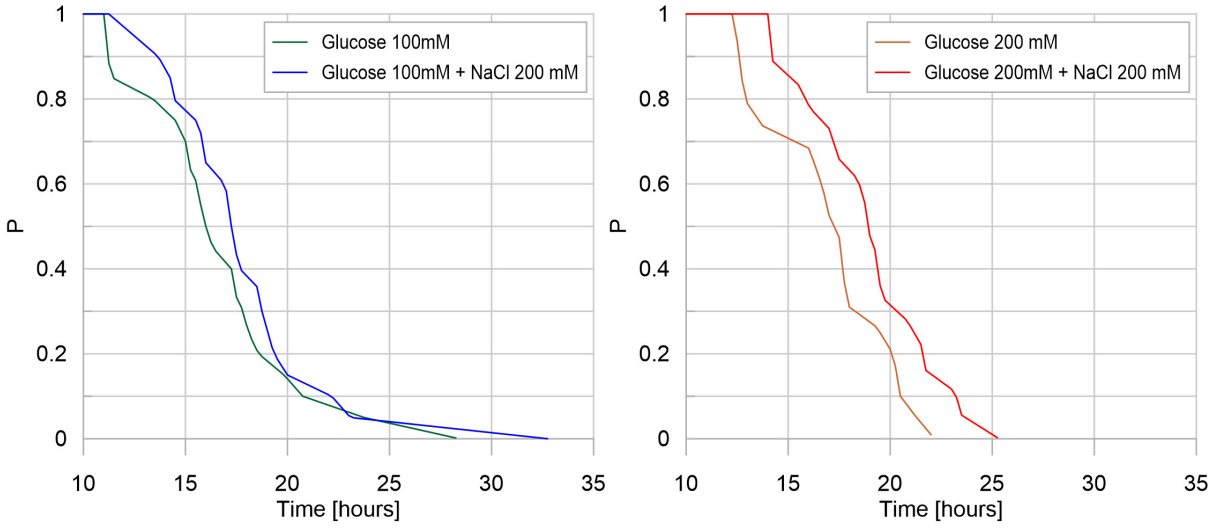

Fig 12. Survival plot: glucose concentration effect. For each treatment, on the vertical axis, the value P corresponds to the fraction of replicates that have not reached the glucose spot at a given time. For a representative number of replicates, P is the probability that glucose has not been reached by slime mold at a given time, for a specific treatment. On the horizontal axis, each value of time corresponds to the average time it takes for a certain fraction of slime mold (P) to reach the glucose spot.

Discussion

Exploration in slime molds involves two different processes: area extension and movement (27). Slime molds locomotion and morphogenesis depend on the response of the organism to the environmental conditions such as light, hygrometry, pH, or the presence of chemicals (29,51). In the present paper, we show that distributions of nutritive and aversive cues affected drastically the exploration pattern of slime molds.

The typical exploration behavior of a slime mold (in control conditions) started by a stretching period where the slime molds grew uniformly in all directions for 10 hours. Then, the contour of slime mold lost circularity when the first pseudopodia appeared, which also corresponds to the first occurrence of mucus. This phenomenon is typical of the directed digitated growth, or branching phase, described by numerous authors (27,52–55). Slime molds developed multiple pseudopodia and did not exhibit any preferential exploration orientation. At the end of the experiment, almost all the arena was explored by the slime mold. Thus the exploration was characterized by three phases: (i) Primary growth only, in the quasi-absence of mucus (5-10 hours); (ii) Combination of primary and secondary growth; (iii) Secondary growth only, when the slime mold stops exploring new substrate areas.

Regarding the result obtained for the homogeneous distribution of nutritive cues, we noted first, an environment containing a uniform distribution of nutrients slowed down the exploration of slime mold, mainly by delaying secondary growth and increasing the period of the pulsatile exploration/refinement movements. The area not explored

413 by the slime molds was 3 times larger (respectively 7 times larger) than in the
414 environment deprived of nutrient (control case) for a slightly nutritive (respectively
415 highly nutritive) environment. The exploration rate was almost linear for highly
416 nutritive environments, while for other treatments, the area covered by the slime
417 molds reached a plateau after a period of stretching, which indicates secondary
418 growth and slime mold displacement. This means that slime molds that explored
419 nutritive environments never exhibited a Phase (iii) in their exploration pattern.
420 Second, on substrates with higher nutrient concentrations, the slime molds grew in a
421 more compact fashion, *i.e*. slime molds presented the highest solidity index and the
422 lowest number of pseudopodia (clusters). Additionally, the appearance of mucus,
423 which indicates that the slime mold was withdrawing, occurred much later in nutritive
424 environments. As glucose is only aversive when only above 300mM (54), our results
425 suggest that nutritive media depressed migration due to feeding behavior. This
426 allows the organism to remain at a site until nutrients are exhausted (56–58). In
427 previous studies, it was shown that the surface area of substrate covered increases
428 when slime mold responds to nutrient dilution (58,59). Here, we confirmed these
429 observations and noted that slime mold tended to migrate and grow faster on
430 substrates with the lowest concentration of nutrients, thus maximizing nutrient intake
431 and optimizing the trade-off between nutrient foraging and nutrient intake.
432
433 Similarly, for a homogeneous distribution of aversive cues we noted the aversion of
434 slime mold to salt manifested itself through longer contemplative behavior, delayed
435 primary growth and a higher probability to crawl on previously explored surface. In
436 addition, the slime molds grew more compactly and with less pseudopods. This
437 suggests that slime molds were actively avoiding contact with the aversive surface

438 (44,50,60). In the absence of cell walls, slime mold has no other protection from the
439 environment than mucus. Indeed, in bacteria for instance, mucus is used as
440 protective barrier for the cells against harsh external conditions (61). In slime molds,
441 the extracellular mucus excreted by the slime molds can have different roles:
442 hydrophilic shield to prevent water loss (62), a lubricating surface over which the
443 slime molds can easily crawl (63), a defensive coat to protect against invasion by
444 foreign materials and organisms (62,64), an aid to phagocytosis (65), a surface that
445 promotes ion-exchange (62) and has externalized spatial memory that helps
446 navigation in unknown environments (26,36,66). Here, we can add a new function for
447 the mucus i.e. a buffer to move in adverse environment. In other words we
448 demonstrate for the first time that the mucus may be used as a safe haven to avoid
449 prolonged and repeated contacts with hazardous substances encountered in the
450 environment.
451
452 Finally, for non-homogeneous distribution of aversive and non-aversive cues, e.g.
453 spot experiments, pulsatile movements were limited and slime molds responded in
454 the same way regardless of the concentration of glucose used as attractant and
455 regardless of the presence of a salt spot on the way to the glucose spot. Slime molds
456 grew in a more compact fashion, *i.e*. slime molds presented the highest solidity index
457 and the lowest number of pseudopodia (clusters). Additionally, the evolution of the
458 areas covered by slime mold and mucus over time indicates that the response of
459 slime molds to heterogeneous environments was similar to that in the control case.
460 This result suggests that in the spot experiments, the exploration behavior of slime
461 mold is mostly controlled by the substrate. Our observation confirms that salt
462 reception can be affected by the presence of sugars (47). The authors in (47)

showed that the “apparent” enthalpy change accompanying salt perception decreases with increase of sugar concentration.

The proposed image analysis program allows extracting information on expansion rates, geometric changes and probability of occupancy. Ongoing developments aim to acquire high quality images of slime mold exploration tests and to expand the code’s capabilities for extracting topological information on the networks formed by slime molds. Slime molds have been shown to be capable of distributed sensing, parallel information processing, and decentralized optimization (39,51,67). It is also viewed by some researchers as an inspiration for bio-computing devices (68–73). Our image analysis methods will help such research avenues by improving data collection.

Trajectories of individuals within a flock could also be described to understand whether or not members of the flock can inform and influence the travel direction of other individuals. Such a finding would allow understanding how group decisions are made among gregarious species (74). The cluster identification and shape recognition program could be used to differentiate modes of gene expression or to recognize objects (75). Object identification is an important pillar to explain associative memory or to track species interactions in an ecosystem. The tools and approach presented here are thus applicable to any problem of network dynamics or pattern recognition (76).

Methods

1) Species

Physarum Polycephalum, also known as the true slime mold, belongs to the Amoebozoa, the sister group to fungi and animals (77). Slime molds are found on organic substrates where they feed on microorganisms such as bacteria or fungi (77). The vegetative morph of *P. polycephalum*, the plasmodium, is a vast multinucleate cell that can grow to cover up to a few square meters and crawl at speeds from 0.1 to few centimeters per hour (29,30). When hygrometry and food availability decrease, the plasmodium turns into an encysted resting stage made of desiccated spherules called sclerotium (29).

2) Rearing conditions

Experiments were initiated with a total of 10 sclerotia per strain (Southern Biological, Victoria, Australia). We cultivated slime molds on a 1% agar medium with rolled oat flakes, slime molds were fed every day and the medium was replaced daily. Slime molds were 2 weeks old when the experiment started. All experiments were carried out in the dark at 25°C temperature and 70% humidity, and ran for 35 h. Pictures were taken with a Canon 70D digital camera.

3) Experimental setup

Initially we monitored the exploration movement evoked in slime molds in a homogeneous environment. Each slime mold was placed in the center of a circular arena (14.5cm in diameter) with a layer of agar (1% in water) mixed with non-nutritive cellulose (5%). Adding cellulose to the agar mix proved to be useful to obtain a homogeneous pigmentation and to enhance the color contrast between the substrate and slime mold, therefore improving the identification process. A circular

hole (2.5cm in diameter) was punched and replaced with a circular slime mold of the same size sitting on oat. In the first and second treatments (nutritive environments) we added glucose (100mM or 200mM) to the medium. In the third treatment (adverse environment), we added a known repellent (NaCl 100mM (55)) to the medium. Lastly, in the fourth treatment, the medium remained unchanged (neutral environment *i.e.* control treatment).

Subsequently, to investigate how chemotaxis modified the exploration behavior, we introduced discrete spots of attractants/repellants within a neutral substrate made of plain agar. In these so-called “spot experiments”, we followed a procedure similar to that for the homogeneous environments. The arena consisted of a 14.5 cm diameter petri dish filled with plain 1% agar mixed with non-nutritive cellulose (5%). Once the agar had set, we punched two or three holes in a line configuration (diameter of each hole 2.5 cm). A circular slime mold (2.5 cm in diameter) was placed diametrically opposite to a glucose (attractant) spot of same size, placed 4.5cm away. In some of the treatments, a salt (NaCl 200mM, repellent) spot was added between the slime mold and the attractant spot. A total of 4 different treatments were tested: the first and the second with a single spot of glucose at concentrations of 100mM and 200mM respectively, the third and fourth keeping the glucose spots with the same concentrations and adding a NaCl 200mM spot. Previous experiments show no disruption of slime mold behavior due top punching alone (45).

All slime molds were fed just before the experiment so we assumed that they were in the same physiological state. The experiment consisted of a total of 8 different treatments. We replicated the experiment 20 times for each treatment and monitored

each arena for 35 hours taking time-lapse photographs every 5 minutes. Fig 13 shows the experimental set-up for homogeneous environments (left) and discrete distributions of attractants/repellants (right).

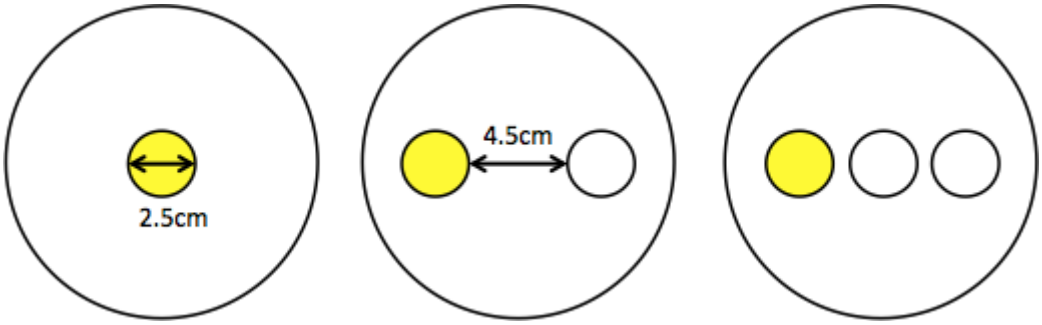

Fig 13: Experimental set-ups for homogenous environment and spot experiment

4) Image Processing

Time-lapse images were taken every 5 minutes for a total of 420 pictures for each replicate. First, the outside of the petri dish was masked by manually identifying the circular contour; then, the images were converted into the ab* color space (which is the CLAB space without the L* lighting component) since this color space yielded better segmentation results. Then, the clustering algorithm k-means (78,79) was used to classify every pixel into one of two categories or clusters: slime mold or not-slime mold. This last category was further refined based on pixel history, becoming either unexplored surface or mucus. Mucus is the substance left by slime after refinement, which acts as an external memory on explored areas (36,66).

The change of class from unexplored substrate to slime mold, defined as primary growth, means that slime mold reached a point it had never explored. Similarly, secondary growth is the change from mucus to slime mold, meaning that the cell is revisiting a location. Lastly, if the slime mold recedes, e.g. a pixel goes from slime

mold to non-slime mold, it becomes mucus, and is defined as refinement. Note that once a pixel is identified as mucus, it can never be classified as unexplored substrate in the following time frames. Two videos are provided as supplementary material, S2 and S3 show one replicate as original images and trinarized images respectively.

5) Image Analysis in Space and Time

We computed indexes to characterize slime mold geometry dynamics and averaged them over the 20 replicates to obtain statistically representative measures. In order to quantify the differences on distinct substrates, we first calculated the fraction of the petri dish area covered by slime mold, mucus and unexplored substrate over time. The total area, the lighting conditions and the test duration were the same for all treatments, both in the homogeneous and spot experiments. Note that glucose only provides energy to slime mold, which is not gaining significant mass during the experiments (58). In other words, slime mold is changing its area by mostly by stretching and contracting, therefore changing its area density.

We then computed the cumulative area of primary growth, refinement, and secondary growth over the full period of the experiments comparing two consecutive images at the time. The cumulative area covered by primary growth is indicative of the total area of exploration, therefore it is always smaller or equal to the total area of the dish. The cumulative area covered by secondary growth indicates whether slime mold expansion is monotonic (dominated by primary growth) which results in a smaller magnitude, or cyclic (secondary growth dominated, with pulsatile movements) which results in a larger magnitude. The cumulative area covered by

583 refinement indicates slime mold density changes. Within a given time interval, if the
584 area covered by primary plus secondary growth equals that covered by refinement,
585 then slime mold keeps the same density, whereas if it is superior, the slime mold
586 stretches (e.g. density decreases). If secondary growth is negligible and if the area
587 covered by primary growth equals the area covered by refinement, then slime mold
588 displaces mass.
589
590 We calculated the extent of growth for each pair of consecutive images as the
591 distance from each pixel where growth occurred (both primary and secondary) to the
592 closest pixel classified as slime mold in the previous image. We calculated the
593 migration rate as the ratio between the maximum extent of growth and the time
594 interval between images (5 min). Then we delineated the region explored by slime
595 mold within the interval as the contour of the slime mold with an offset distance
596 corresponding to the migration rate (see the supplementary material Fig 1 in S1
597 Appendix for more details).
598
599 We estimated the fraction of secondary growth relative to the total number of pixels
600 in the region of expansion. We then calculated the fraction of “expected secondary
601 growth”, which would have occurred if secondary growth had happened randomly. If
602 the measured secondary growth fraction is higher (respectively, lower) than the
603 expected one, this means that slime mold has a bias towards mucus (respectively,
604 unexplored substrate).
605

606 Additionally, we computed four shape parameters indicative of the contour of slime
607 mold: circularity, eccentricity, solidity and number of clusters. Circularity (C) is
608 defined as:

$$C = {P^2}/{4\pi A}$$

609 Where P and A are the perimeter and area of the shape of slime mold at a given
610 time. Eccentricity (E) is calculated as the ratio between the distance between the foci
611 and the major axis length, as follows:

$$E = \sqrt{1 - \left(\frac{b}{a}\right)^2}$$

612 In which *a* and *b* are the lengths of the major and minor axes, respectively. Solidity
613 (S) is the ratio between the area of the slime mold contour and the area of its convex
614 hull. Lastly, we measured the number of clusters by performing an erosion operation
615 along the contour of slime mold, after which only the clusters of high concentration of
616 slime mold remain, which provided the number of pseudopodia or clusters of slime
617 mold.
618
619 For the spot experiments, we also determined the distance from the slime mold to
620 the glucose spot at every time, as the minimum distance between the contour of
621 slime mold and the glucose spot. The evolution of the distance to glucose over time
622 was analyzed in a way similar to a survival analysis.
623
624 **6) Statistics**
625
626 The full description of the statistics is provided as part of the supplementary
627 information; appendix S1 includes the statistical procedure and results; while

appendix S4 is an R markdown allowing analysis reproduction. When dependent variables lasted until the occurrence of certain event, we conducted survival analyses using the R package coxme (80). For the remaining dependent variables, we did linear analyses using the R packages lme4 (81) and lmerTest (82). We tested as fixed factors the four treatments in the homogeneous experiment and both the attracting and the repelling spots and their interaction. The date of the experiment was considered as a random factor. Finally, we performed a nested model comparison using the R package MuMIn (83) by ordering models according to their Akaike criterion and represented the selected model by plotting each estimator, their 95%CI and p-values.

Supporting information

S1 Appendix. Supplementary information: Image analysis and statistical results. Description of the methodology to extract indexes from image analysis and results obtained from the statistical analysis that support our observations**.**

S2 Video. Time-lapse of one experiment replicate, original images. Video showing the evolution of the slime mold cell over the 35 hours of the experiments, original acquired photos.

S3 Video. Time-lapse of one experiment replicate, trinarized images. Time lapse of the results of the image segmentation for the same experiment shown in S2 Video.

S4 Appendix. Statistical analysis script description. Step by step description of the procedure followed to generate the results of the shown statistical analyses.

Acknowledgements

This work was supported by the U.S National Science Foundation, under grant CMMI#1552368: “CAREER: Multiphysics Damage and Healing of Rocks for Performance Enhancement of Geo-Storage Systems - A Bottom-Up Research and Education Approach.” A.D. and A.B. were supported by a grant from the Agence Nationale de la Recherche (reference number: ANR-17-CE02-0019-01 -SMART-CELL).

The authors declare no competing interests.

References

1. Ball P, Borley NR. The self-made tapestry: pattern formation in nature. Vol. 198. Oxford University Press Oxford; 1999.
2. Rietkerk M, de Koppel J. Regular pattern formation in real ecosystems. Trends Ecol Evol. 2008;23(3):169–75.
3. Theraulaz G, Gautrais J, Camazine S, Deneubourg J-L. The formation of spatial patterns in social insects: from simple behaviours to complex structures. Philos Trans R Soc London Ser A Math Phys Eng Sci. 2003;361(1807):1263–82.
4. Teague BP, Guye P, Weiss R. Synthetic morphogenesis. Cold Spring Harb Perspect Biol. 2016;8(9):a023929.
5. Goodwin BC. Unicellular morphogenesis. Cell Shape Determ Regul Regul Role. 1989;365–91.
6. Chalut KJ, Paluch EK. The actin cortex: a bridge between cell shape and function. Dev Cell. 2016;38(6):571–3.
7. Driscoll MK, McCann C, Kopace R, Homan T, Fourkas JT, Parent C, et al. Cell shape dynamics: from waves to migration. PLoS Comput Biol. 2012;8(3):e1002392.
8. Salbreux G, Charras G, Paluch E. Actin cortex mechanics and cellular morphogenesis. Trends Cell Biol. 2012;22(10):536–45.
9. Charras G, Sahai E. Physical influences of the extracellular environment on cell migration. Nat Rev Mol cell Biol. 2014;15(12):813.

10. van Helvert S, Storm C, Friedl P. Mechanoreciprocity in cell migration. Nat Cell Biol. 2018;20(1):8.
11. Friedl P, Wolf K. Plasticity of cell migration: a multiscale tuning model. J Cell Biol. 2010;188(1):11–9.
12. Gardel ML, Schneider IC, Aratyn-Schaus Y, Waterman CM. Mechanical integration of actin and adhesion dynamics in cell migration. Annu Rev Cell Dev Biol. 2010;26:315–33.
13. Inagaki N, Katsuno H. Actin waves: Origin of cell polarization and migration? Trends Cell Biol. 2017;27(7):515–26.
14. Aman A, Piotrowski T. Cell migration during morphogenesis. Dev Biol. 2010;341(1):20–33.
15. Reig G, Pulgar E, Concha ML. Cell migration: from tissue culture to embryos. Development. 2014;141(10):1999–2013.
16. Yamada KM, Mayor R. Cell dynamics in development, tissue remodelling, and cancer. Curr Opin Cell Biol. 2016;42:iv.
17. Hind LE, Vincent WJB, Huttenlocher A. Leading from the back: the role of the uropod in neutrophil polarization and migration. Dev Cell. 2016;38(2):161–9.
18. Mseka T, Bamburg JR, Cramer LP. ADF/cofilin family proteins control formation of oriented actin-filament bundles in the cell body to trigger fibroblast polarization. J Cell Sci. 2007;120(24):4332–44.
19. King JS, Insall RH. Chemotaxis: finding the way forward with Dictyostelium. Trends Cell Biol. 2009;19(10):523–30.
20. Iglesias PA, Devreotes PN. Navigating through models of chemotaxis. Curr Opin Cell Biol. 2008;20(1):35–40.
21. Larsen SH, Adler J, Gargus JJ, Hogg RW. Chemomechanical coupling without

727 ATP: the source of energy for motility and chemotaxis in bacteria. Proc Natl
728 Acad Sci. 1974;71(4):1239–43.
729 22. Nakaoka Y, Iwatsuki K. Hyperpolarization-activated inward current associated
730 with the frequency increase in ciliary beating of Paramecium. J Comp Physiol
731 A. 1992;170(6):723–7.
732 23. Saranak J, Foster KW. Rhodopsin guides fungal phototaxis. Nature.
733 1997;387(6632):465.
734 24. Nakagaki T, Yamada H, Tóth A. Maze-solving by an amoeboid organism.
735 Nature [Internet]. 2000;407(6803):470. Available from:
736 http://www.ncbi.nlm.nih.gov/pubmed/11028990
737 25. Kuroda S, Takagi S, Nakagaki T, Ueda T. Allometry in Physarum plasmodium
738 during free locomotion: size versus shape, speed and rhythm. J Exp Biol.
739 2015;218(23):3729–38.
740 26. Rodiek B, Hauser MJB. Migratory behaviour of Physarum polycephalum
741 microplasmodia. Eur Phys J Spec Top. 2015;224(7):1199–214.
742 27. Vogel D, Nicolis SC, Perez-Escudero A, Nanjundiah V, Sumpter DJT,
743 Dussutour A. Phenotypic variability in unicellular organisms: from calcium
744 signalling to social behaviour. Proc R Soc B Biol Sci.
745 2015;282(1819):20152322.
746 28. Vogel D, Dussutour A, Deneubourg J-L. Symmetry breaking and inter-clonal
747 behavioural variability in a slime mould. Biol Lett. 2018;14(12):20180504.
748 29. Aldrich H. Cell biology of Physarum and Didymium V1: organisms, nucleus,
749 and cell cycle. Elsevier; 2012.
750 30. Oettmeier C, Brix K, Döbereiner H-G. Physarum polycephalum—A new take
751 on a classic model system. J Phys D Appl Phys. 2017;50(41):413001.

752 31. Ueda T. Pattern dynamics in cellular perception. Phase Transitions A Multinatl
753 J. 1993;45(2–3):93–104.
754 32. Kuroda R, Kuroda H. Relation of cytoplasmic calcium to contractility in
755 Physarum polycephalum. J Cell Sci. 1982;53(1):37–48.
756 33. Yoshimoto Y, Matsumura F, Kamiya N. Simultaneous oscillations of Ca2+
757 efflux and tension generation in the permealized plasmodial strand of
758 Physarum. Cell Motil. 1981;1(4):433–43.
759 34. Farr DR, Amster H, Horisberger M. Composition and partial structure of the
760 extracellular polysaccharide of Physarum polycephalum. Carbohydr Res.
761 1972;24(1):207–9.
762 35. Sesaki H, Ogihara S. Secretion of slime, the extracellular matrix of the
763 plasmodium, as visualized with a fluorescent probe and its correlation with
764 locomotion on the substratum. Cell Struct Funct. 1997;22(2):279–89.
765 36. Reid CR, Latty T, Dussutour A, Beekman M. Slime mold uses an externalized
766 spatial “memory” to navigate in complex environments. Proc Natl Acad Sci.
767 2012;109(43):17490–4.
768 37. Reid CR, Beekman M. Solving the Towers of Hanoi - how an amoeboid
769 organism efficiently constructs transport networks. J Exp Biol [Internet].
770 2013;216:1546–51. Available from:
771 http://www.ncbi.nlm.nih.gov/pubmed/23307798
772 38. Ueda T, Hirose T, Kobatake Y. Membrane biophysicsdf chemoreception and
773 taxis in the plasmodium of physarum polycephalum. Biophys Chem.
774 1980;11(3–4):461–73.
775 39. Reid CR, Latty T. Collective behaviour and swarm intelligence in slime moulds.
776 FEMS Microbiol Rev. 2016;40(6):798–806.

40. Saigusa T, Tero A, Nakagaki T, Kuramoto Y. Amoebae anticipate periodic events. Phys Rev Lett. 2008;100(1):18101.
41. Tero A, Takagi S, Saigusa T, Ito K, Bebber DP, Fricker MD, et al. Rules for biologically inspired adaptive network design. Science [Internet]. 2010 Jan 22 [cited 2018 Nov 21];327(5964):439–42. Available from: http://www.ncbi.nlm.nih.gov/pubmed/20093467
42. Latty T, Beekman M, Biernaskie J, Walker S, Gegear R, Boivin G, et al. Slime moulds use heuristics based on within-patch experience to decide when to leave. J Exp Biol [Internet]. 2015;218(Pt 8):1175–9. Available from: http://www.ncbi.nlm.nih.gov/pubmed/25722006
43. Reid CR, Garnier S, Beekman M, Latty T. Information integration and multiattribute decision making in non-neuronal organisms. Anim Behav. 2015;100:44–50.
44. Boisseau RP, Vogel D, Dussutour A. Habituation in non-neural organisms: evidence from slime moulds. Proc R Soc B Biol Sci. 2016;283(1829):20160446.
45. Dussutour A, Ma Q, Sumpter D. Phenotypic variability predicts decision accuracy in unicellular organisms. Proc R Soc B. 2019;286(1896):20182825.
46. Adamatzky A. Slime Mold Solves Maze in One Pass, Assisted by Gradient of Chemo-Attractants. IEEE Trans Nanobioscience [Internet]. 2012 Jun [cited 2019 Aug 8];11(2):131–4. Available from: http://ieeexplore.ieee.org/document/6148283/
47. Terayama K, Ueda T, Kurihara K, Kobatake Y. Effect of sugars on salt reception in true slime moldPhysarum polycephalum. J Membr Biol. 1977;34(1):369–81.

802 48. Carlile MJ. Nutrition and chemotaxis in the myxomycete Physarum
803 polycephalum: the effect of carbohydrates on the plasmodium. Microbiology.
804 1970;63(2):221–6.
805 49. Ueda T, Terayama K, Kurihara K, Kobatake Y. Threshold phenomena in
806 chemoreception and taxis in slime mold Physarum polycephalum. J Gen
807 Physiol. 1975;65(2):223–34.
808 50. Ueda K, Takagi S, Nishiura Y, Nakagaki T. Mathematical model for
809 contemplative amoeboid locomotion. Phys Rev E. 2011;83(2):21916.
810 51. Jones J. Characteristics of Pattern Formation and Evolution in Approximations
811 of Physarum Transport Networks. Artif Life [Internet]. 2010 Apr [cited 2019 Aug
812 8];16(2):127–53. Available from:
813 http://www.ncbi.nlm.nih.gov/pubmed/20067403
814 52. Halvorsrud R, Wagner G. Growth patterns of the slime mold Physarum on a
815 nonuniform substrate. Phys Rev E. 1998;57(1):941.
816 53. Nakagaki T, Yamada H, Ueda T. Interaction between cell shape and
817 contraction pattern in the Physarum plasmodium. Biophys Chem.
818 2000;84(3):195–204.
819 54. Latty T, Beekman M. Food quality affects search strategy in the acellular slime
820 mould, Physarum polycephalum. Behav Ecol. 2009;20(6):1160–7.
821 55. Vogel D, Dussutour A. Direct transfer of learned behaviour via cell fusion in
822 non-neural organisms. Proc R Soc B Biol Sci. 2016;283(1845):20162382.
823 56. Knowles DJC, Carlile MJ. The chemotactic response of plasmodia of the
824 myxomycete Physarum polycephalum to sugars and related compounds.
825 Microbiology. 1978;108(1):17–25.
826 57. Daniel JW, Baldwin HH. Methods of culture for plasmodial myxomycetes. In:

827 Methods in Cell Biology. Elsevier; 1964. p. 9–41.
828 58. Dussutour A, Latty T, Beekman M, Simpson SJ. Amoeboid organism solves
829 complex nutritional challenges. Proc Natl Acad Sci. 2010;107(10):4607–11.
830 59. Takamatsu A, Takaba E, Takizawa G. Environment-dependent morphology in
831 plasmodium of true slime mold Physarum polycephalum and a network growth
832 model. J Theor Biol. 2009;256(1):29–44.
833 60. Adamatzky A. Routing Physarum with repellents. Eur Phys J E [Internet]. 2010
834 Apr 17 [cited 2019 Aug 8];31(4):403–10. Available from:
835 http://link.springer.com/10.1140/epje/i2010-10589-y
836 61. Nwodo U, Green E, Okoh A. Bacterial exopolysaccharides: functionality and
837 prospects. Int J Mol Sci. 2012;13(11):14002–15.
838 62. McCormick JJ, Blomquist JC, Rusch HP. Isolation and characterization of a
839 galactosamine wall from spores and spherules of Physarum polycephalum. J
840 Bacteriol. 1970;104(3):1119–25.
841 63. Simon HL, Henney HR. Chemical composition of slime from three species of
842 myxomycetes. FEBS Lett. 1970;7(1):80–2.
843 64. Asgari M, Henney JHR. Inhibition of growth and cell wall morphogenesis of
844 Bacillus subtilis by extracellular slime produced by Physarum flavicomum.
845 Cytobios. 1977;20(79–80):163–77.
846 65. Haskins EF, Hinchee AA. Light-and ultra-microscopical observations on the
847 surface structure of the protoplasmodium, aphanoplasmodium, and
848 phaneroplasmodium (Myxomycètes). Can J Bot. 1974;52(8):1835–9.
849 66. Reid CR, Beekman M, Latty T, Dussutour A. Amoeboid organism uses
850 extracellular secretions to make smart foraging decisions. Behav Ecol.
851 2013;24(4):812–8.

67. Adamatzky A. Physarum Machines [Internet]. WORLD SCIENTIFIC; 2010 [cited 2019 Aug 8]. (World Scientific Series on Nonlinear Science Series A; vol. 74). Available from: https://www.worldscientific.com/worldscibooks/10.1142/7968
68. Adamatzky A. Advances in physarum machines : sensing and computing with slime mould. 1st edition 2016. Springer International Publishing : Imprint: Springer,; 2016. 839 p. (Emergence, Complexity and Computation,).
69. SCHUMANN A, ADAMATZKY A. PHYSARUM SPATIAL LOGIC. New Math Nat Comput [Internet]. 2011 Sep 21 [cited 2019 Aug 8];07(03):483–98. Available from: https://www.worldscientific.com/doi/abs/10.1142/S1793005711002037
70. Adamatzky A. Physarum machines: encapsulating reaction–diffusion to compute spanning tree. Naturwissenschaften [Internet]. 2007 Nov 14 [cited 2019 Aug 8];94(12):975–80. Available from: http://www.ncbi.nlm.nih.gov/pubmed/17603779
71. Adamatzky A, Jones J. Towards Physarum Robots: Computing and Manipulating on Water Surface. J Bionic Eng [Internet]. 2008 Dec 1 [cited 2019 Aug 8];5(4):348–57. Available from: https://www.sciencedirect.com/science/article/pii/S1672652908601808
72. Adamatzky A, Martínez GJ, Chapa-Vergara S V., Asomoza-Palacio R, Stephens CR. Approximating Mexican highways with slime mould. Nat Comput [Internet]. 2011 Sep 28 [cited 2019 Aug 8];10(3):1195–214. Available from: http://link.springer.com/10.1007/s11047-011-9255-z
73. Umedachi T, Takeda K, Nakagaki T, Kobayashi R, Ishiguro A. Fully decentralized control of a soft-bodied robot inspired by true slime mold. Biol

877 Cybern [Internet]. 2010 Mar 4 [cited 2019 Aug 8];102(3):261–9. Available from:
878 http://link.springer.com/10.1007/s00422-010-0367-9
879 74. Couzin ID. Collective cognition in animal groups. Trends Cogn Sci.
880 2009;13(1):36–43.
881 75. Olshausen BA, Anderson CH, Van Essen DC. A neurobiological model of
882 visual attention and invariant pattern recognition based on dynamic routing of
883 information. J Neurosci. 1993;13(11):4700–19.
884 76. Tamayo P, Slonim D, Mesirov J, Zhu Q, Kitareewan S, Dmitrovsky E, et al.
885 Interpreting patterns of gene expression with self-organizing maps: methods
886 and application to hematopoietic differentiation. Proc Natl Acad Sci.
887 1999;96(6):2907–12.
888 77. Stephenson SL, Schnittler M. Myxomycetes. Handb Protists. 2017;1405–31.
889 78. Kanungo T, Mount DM, Netanyahu NS, Piatko CD, Silverman R, Wu AY. An
890 efficient k-means clustering algorithm: Analysis and implementation. IEEE
891 Trans Pattern Anal Mach Intell. 2002;(7):881–92.
892 79. Dhanachandra N, Manglem K, Chanu YJ. Image Segmentation Using K -
893 means Clustering Algorithm and Subtractive Clustering Algorithm. Procedia
894 Comput Sci [Internet]. 2015 Jan 1 [cited 2019 Aug 8];54:764–71. Available
895 from: https://www.sciencedirect.com/science/article/pii/S1877050915014143
896 80. Therneau T. A Package for Survival Analysis in S. version 2.38. 2015.
897 81. Bates D, Sarkar D, Bates MD, Matrix L. The lme4 package. R Packag version.
898 2007;2(1):74.
899 82. Kuznetsova A, Brockhoff PB, Christensen RHB. lmerTest package: tests in
900 linear mixed effects models. J Stat Softw. 2017;82(13).
901 83. Barton K, Barton MK. Package 'MuMIn'Version 1. 2015;

Author Contribution Statement

Author Fernando Patino-Ramirez (FP) carried out the image analysis, wrote the corresponding sections about methods and results created the figures in the manuscript and was responsible of the image analysis section on S1 and the videos S2 and S3. AB developed the statistical analysis, including the corresponding sections in supplementary materials S1 and S4. Authors Aurèle Boussard (AB) and Audrey Dussutour (AD) carried out the experiments in the laboratory and the corresponding image acquisition. Chloé Arson (CA) drafted the manuscript and contributed in the planning, analysis and interpretation of the experiments and the data together with AD, FP and AB.

All the authors have approved the submitted version of this manuscript and have agreed both to be accountable for the author's own contributions.